Numerical Modeling of Flow Characteristics for A Reach Reach from Damietta Branch Using K-ε Turbulence Model

نمذجة عددية لخصائص السريان لحبس من فرع دمياط بإستخدام نموذج الإضطراب K-ε

Zidan, A.A.[1], El-Alfy, K.S.[2], Abdalla, M.G. [3] and El-Gamal, M.I.[4]

1, 2: Prof. of hydraulics, Irrigation and Hydraulics Dept., Faculty of Eng., El-Mansoura University

3: Associate prof., Irrigation and Hydraulics Dept., Faculty of Eng., El-Mansoura University

4: Assistant lecturer, Irrigation and Hydraulics Dept., Faculty of Eng., El-Mansoura University

خلاصة:

في هذا البحث تم عمل نمذجة عددية لخصائص السريان لحبس منحني من فرع دمياط وذلك بإستخدام نموذج ثلاثي الأبعاد يسمي (IRIC) . تهدف هذه الدراسة إلي تحديد المناطق الأكثر عرضة لعملية النحر في هذا الحبس نتيجة تأثرها بالسرعات العالية حتي يمكن وضع حلول عملية لحمايتها. يبلغ طول الحبس تحت الدراسة حوالي 6.78 كم من الكيلو 95.22 إلي الكيلو 102 خلف محطة مقياس الروضة. حللت البيانات الحقلية اللازمة لعملية الدراسة. تم إستخدام طريقة الفروق المحدودة الصريحة في هذا النموذج وحققت نتائج النموذج بإستخدام البيانات الحقلية المشار إليها. من أجل الوصول إلي نتائج قريبة من الواقع في عملية النمذجة ، تم تطبيق نموذج الإضطراب القياسي (k-ε) . إستخدمت طريقة (Upwind scheme) لحل أجزاء الإنتقال في معادلات الحركة مع الإفتراض بحركة رسوبيات القاع فقط وأن إتجاهها هو نفس إتجاه السريان . في هذا البحث تم دراسة تأثير النباتات المتواجدة علي حركة السريان وكذلك التداخل بين تلك النباتات وحركة الرسوبيات. أوضحت الدراسة أن الحركة الدوامية في الجزء الأمامي المنحني من الحبس أكبر منها في المنحني الخلفي نتيجة لشدة الإنحناء الأمامي ، نتج عنها زيادة السرعات في الجزء الأمامي مما قد يسبب الزيادة في عملية النحر.

ABSTRACT

In this research, a meandering reach from Damietta branch was selected and numerically studied. The aim of this study is to find the vulnerable zones subjected to maximum velocities so as to assign the appropriate methodology of training structures for improving and stabilizing flow conditions. This reach is approximately 6.78 km long, which located between km 95.22 and km 102 downstream of El- Roda gauge station. Field data were collected and analyzed for the modeling process. A 3-D model called IRIC (International River Interface Corporative) based on an explicit finite difference method (Abbott-Ionescu scheme) was applied. Therefore, in order to fulfill such objective, K-ε turbulence model was employed using upwind scheme of the advection terms. Through the modeling process, it was assumed that the sediment particles move in the bed layer zone only and the direction of sediment transport is the same as direction of flow. The effect of vegetation and interactions between sediment motion and vegetation were added in the modeling process. This model treats vegetation drag effects explicitly through drag terms in the equations of motion. From this study, it was found that the vorticity values through the upstream curve are greater than the corresponding ones in the downstream curve; consequently, the upstream curve is subjected to high water velocity values which may increase the scouring process.

Key words: Numerical modeling, Turbulence model, Sediment, Vegetation, K-ε model

1. INTRODUCTION

Flow in curved river reaches is usually under the influence of centrifugal acceleration, which induces transverse velocity component (helical flow currents) and super elevation in water surface. Although, these curved reaches are sometimes stable, there are general tendency of bank failure and bed scour at the outer bend followed by sedimentation at the inner bend. Therefore, lateral migration of the reach planform occurs, consequently several morphological and navigational problems take place. Due to these dynamic interactions, the transverse velocity profile, shear stress on channel bed, lateral bed slope, sediment size distribution, and energy expenditure will be changed (Grade, 1995).

A meander is a bend in a sinuous watercourse or river. It is formed when the moving water in a stream erodes the outer banks and widens its valley. A stream of any size could be assumed a meandering course, alternately eroding sediment from the outside of a bend and depositing them on the inside. The result is a snaking pattern as the stream meanders back and forth across its down-valley axis. When a meander gets cut off from the main stream, an oxbow lake is formed. Over time meanders migrate downstream, sometimes in such a short time, creating civil engineering problems for local municipalities who attempt to maintain stable roads and bridges (Hickin, 2003).

Stable alluvial river in natural state tends to maintain water conveyance of a specific magnitude by managing its sediment movement and deposition. Variation in local sedimentation, valley slope, geologic properties, and hydrograph influence its geometry as well as the arrangement of the sediment. Therefore, river meandering, lateral migration, deterioration of local navigation depths and flood conveyance are the result of the movement and deposition of bed sediment.

Attia and El-Saied (2004) investigated the statistical nature of river bends along Damietta branch. In this study, three bend types were defined as: free, limited, and forced; which were classified according to the physical and morphological characteristics and degree of freedom to attain the lateral shifting. They concluded that Damietta branch is changing in its planform several times down its course. Also, they summarized meander dimensions of many investigators such as given by Inglis (1938), Leoplod and Wolman (1960, 1964) and Zeller (1967). Based on the analytical regression of the non-linear relationships, there study derived many formulas for Damietta branch concerning the three mentioned types of bends. These formulas linked different parameters of meander geometrical sizes (Ahmed, 2010).

As the combined transport of water and sediment in rivers is a complex process, on-site investigations, evaluation of experience and large scale prototype tests are needed for verifying the results obtained from any mathematical or physical models.

For computation of the bed formation in river bends or near bifurcations, it is important to develop one dimensional models to be two dimensional models. In such models, the two dimensional flow equations in the x and y directions are used.

Three dimensional models need long time and large cost in computations (Wang, 1988; Wang et al., 1989; and Shimizu et al., 1990). In these models the state of turbulence is characterized by turbulence models such as standard k-ε, RNG k- ε and zero equation models.

The aim of this research is to determine accurately the zones subjected to maximum water velocities and scouring

processes in a selected reach so as to find the suitable structure used for improving flow conditions at the curves of this reach.

2. FIELD WORK

• Site Description

As Damietta branch is very well concerned by Ministry of Water Resources and Irrigation and Ministry of Transport, Egypt, for passing maximum required discharges as well as to develop such safe navigation waterway, the study reach under consideration was selected. The reach was selected in such a way to consist two successive meandering curves where point bars and pools are the dominant bed forms and composed of a relatively homogeneous combination of fine sand and silt. This reach is approximately 6.869 km long which locates from km 69.219 to km 76.088 downstream of Delta Barrages, Damietta branch, i.e. from km 95.22 to km 102 downstream of El- Roda gauge station, Fig. (1). *Fig. (1): Location of the study reach.*

3D Model View for the reach under study
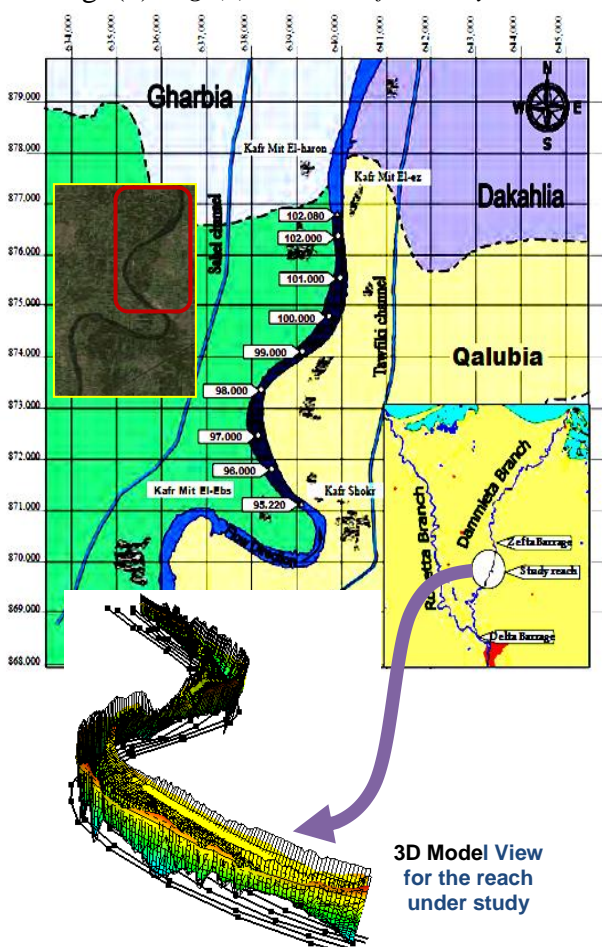
• Field Data Collection

The hydrographic survey of the study reach was carried out by Hydraulics Research Institute "HRI" of the National Water Research Center, Ministry of water resources and Irrigation, Egypt. Using the provided echo-sounder light boat, riverbed bathymetric survey was carried out along the branch following zigzag pathway trans-sections between the two river sides which are roughly spaced at 50 m intervals in stream wise direction. Moreover, in order to cover the study reach area, three longitudinal sections located at the left, middle, and right sides of the river reach were acquired.

Consequently, the provided differential Global Positioning System (GPS), Plates (1) and (2), were employed to record each data set point consisting of X and Y positions as well as the flow depth at an interval of one second on the equipped data logger.
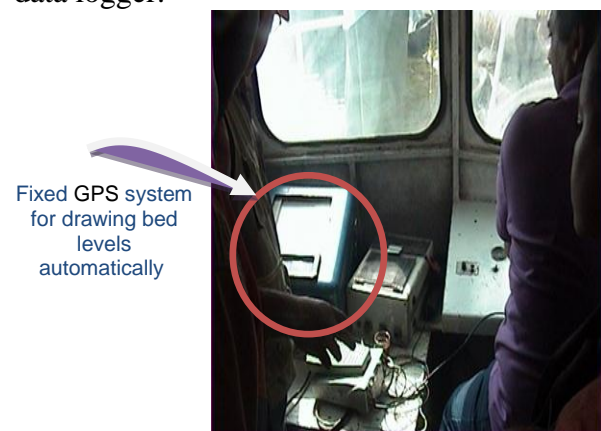

Fixed GPS system for drawing bed levels automatically

Plate (1): *Differential GPS system fixed in echo-sounder light boat.*

Movable GPS System used for determining X and Y coordinates according to global coordinates

Plate (2): *Movable GPS used for measuring the coordinates along sides.*

Due to the significance of the acquired measurements, differential GPS system was utilized to provide a global accuracy of nearly 1.0 m in the plan direction with a relative depth accuracy of +/-10 cm. While the applied echo-sounder system permits flow depth measurements and consequently determining bed elevation with a relative accuracy of +/- 5 cm. For shallow areas, where the flow depths are less than 0.75 m, another total station system was used which was launched on a light rubber boat (Zodiac). Then, the file of these coordinates (X, Y and Z coordinates) was prepared in the form of (XYZ.tpo) file that would be required for the 3D simulation.

The velocity measurements were carried out at locations of 0.606 km, 3.784 km and 6.617 km from the upstream boundary of the reach under study which is located downstream km 95.22.

The grab sediment sampler was used to collect 17 bed material samples at different locations to prepare (d_{50}.anc) file used for the 3-D modeling process. The bed sample locations were selected to cover the entire features of the study reach and to represent the difference in the value of the Manning roughness. The samples were analyzed for grain size distribution, according to the relevant specifications, in the Hydraulics Research Institute.

Eight years data between 2005 and 2012 were collected downstream of Delta barrages, for estimating the maximum and minimum discharges.

The required discharges used for the modeling processes are:

•**The measured discharge** (35.50 M. m³/day): is the measured flow discharge during field measurements which equals to 35.50 million m³/day.

•**The minimum flow discharge** (9.90 M. m³/day): is the minimum recorded value downstream of Delta barrages throughout the

studied years on January 2010, though not being the least value, it is considered the least adequate discharge case for irrigation and navigation;

•**The maximum flow discharge** (62.10 M. m³/day): is the maximum recorded value downstream of Delta barrages throughout the investigated years; and

•**The future discharge values (1 and 2)** (80 M. m³/day and 120 M. m³/day): which are stated by the Nile Research Institute as future peak discharges for Damietta branch rehabilitation.

3. MODEL SET UP

• Governing Equations

• *Momentum equation in X-direction*

$$\frac{\partial(uh)}{\partial t} + \frac{\partial(u^2 h)}{\partial x} + \frac{\partial(uvh)}{\partial y} = -gh\frac{\partial H}{\partial x} - \frac{\tau_x}{\rho} + D_x \quad (1)$$

• *Momentum equation in Y-direction*

$$\frac{\partial(vh)}{\partial t} + \frac{\partial(v^2 h)}{\partial y} + \frac{\partial(uvh)}{\partial x} = -gh\frac{\partial H}{\partial y} - \frac{\tau_y}{\rho} + D_y \quad (2)$$

• *Continuity Equation*

$$\frac{\partial(h)}{\partial t} + \frac{\partial(vh)}{\partial y} + \frac{\partial(uh)}{\partial x} = 0.0 \quad (3)$$

where:

v : velocity in Y-direction;
u : velocity in X-direction;
τ_x : shear stress at X-direction;
τ_y : shear stress at Y-direction;
t : time;
h : water depth at any point;
ρ : water density; and
g : gravitational acceleration.

The governing equations were converted from co-orthogonal coordinates (X and Y coordinates) to represent the local stream lines into river coordinates, non-orthogonal coordinate system, (general coordinates or

ξ and η coordinates). The non-orthogonal coordinate system allows more precise fitting of the coordinate system to suit arbitrary channel curvature and variable width. More importantly, the more detailed treatment of turbulence and large eddies allow predictions of time-variable behavior even for steady discharges.

• Standard K-ε Turbulence Model

Turbulent flow is dissipative, which means that kinetic energy in the small dissipative eddies are transformed into internal energy. The small eddies receive the kinetic energy from slightly larger eddies. The slightly larger eddies receive their energy from even larger eddies and so on. The largest eddies extract their energy from the mean flow. This process of transferred energy from the largest turbulent scales (eddies) to the smallest is called *cascade process*.

This model is represented by the following equations:

$$\upsilon = C_\mu \frac{k^2}{\varepsilon} \tag{4}$$

$$\frac{\partial k}{\partial t} + u\frac{\partial k}{\partial x} + v\frac{\partial k}{\partial y} = \frac{\partial}{\partial x}\left(\frac{\upsilon}{\sigma k}\frac{\partial k}{\partial x}\right) + \frac{\partial}{\partial y}\left(\frac{\upsilon}{\sigma k}\frac{\partial k}{\partial y}\right)$$
$$+ P_h + P_{k\upsilon} - \varepsilon \tag{5}$$

$$\frac{\partial \varepsilon}{\partial t} + u\frac{\partial \varepsilon}{\partial x} + v\frac{\partial \varepsilon}{\partial y} = \frac{\partial}{\partial x}\left(\frac{\upsilon}{\sigma \varepsilon}\frac{\partial \varepsilon}{\partial x}\right) + \frac{\partial}{\partial y}\left(\frac{\upsilon}{\sigma \varepsilon}\frac{\partial \varepsilon}{\partial y}\right)$$
$$+ C_{1\varepsilon}\frac{\varepsilon}{k}P_h + P_{\varepsilon\upsilon} - C_{2\varepsilon}\frac{\varepsilon^2}{k} \tag{6}$$

where:

υ : eddy viscosity;
u : water velocity in X-direction;
v : water velocity in Y-direction;
k : turbulence kinetic energy;
ε : turbulence dissipation; and
t : time.

and,

$$P_h = \upsilon\left[2\left(\frac{\partial u}{\partial x}\right)^2 + 2\left(\frac{\partial v}{\partial y}\right)^2 + \left(\frac{\partial u}{\partial y} + \frac{\partial v}{\partial x}\right)^2\right] \tag{7}$$

$$P_{kv} = C_k\frac{u_*^3}{h}, \quad P_{\varepsilon\upsilon} = C_\varepsilon\frac{u_*^4}{h^2} \tag{8}$$

$$u_* = \sqrt{C_f\left(u^2 + v^2\right)} \tag{9}$$

$$C_k = \frac{1}{\sqrt{C_f}}, C_\varepsilon = 3.6\frac{C_{2\varepsilon}}{C_f^{\frac{3}{4}}}\sqrt{C\mu} \tag{10}$$

where,

Cμ	C$_{1\varepsilon}$	C$_{2\varepsilon}$	σk	σε
0.09	1.44	1.92	1.0	1.30

• Sediment Transport Model

In general, it is assumed that the direction of sediment transport is the same as direction of flow, Fig. (2).

The general modeling equation is:

$$\frac{\partial z_b}{\partial t} + \frac{1}{1-\lambda}\left(\frac{\partial q_{bx}}{\partial x} + \frac{\partial q_{by}}{\partial y}\right) = 0.0 \tag{11}$$

where:

Z_b : elevation of bed;
t : time;
λ : porosity of sediment mixture;
q_{bx} : sediment rate in X-direction; and
q_{by} : sediment rate in Y-direction.

Streamline ≈ direction of flow
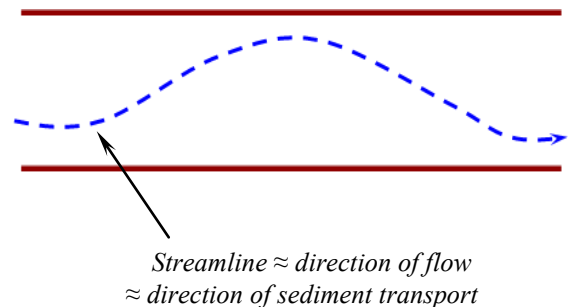*≈ direction of sediment transport*

Fig. (2): *Definition sketch shows the direction of sediment transport.*

Watanabe gave the following equations for the sediment transport rates in X and Y directions as (Shimizu, 2012):

$$q_{bx} = q_b \left[\frac{u_b}{V_b} - \gamma \left(\frac{\partial z_b}{\partial x} + \cos \theta s \frac{\partial z_b}{\partial y} \right) \right] \quad (12)$$

$$q_{by} = q_b \left[\frac{v_b}{V_b} - \gamma \left(\frac{\partial z_b}{\partial y} + \cos \theta s \frac{\partial z_b}{\partial x} \right) \right] \quad (13)$$

according to Hasegwa's formula,

$$\gamma = \sqrt{\frac{1}{\mu_s \, \mu_k}} \quad (14)$$

where:

μ_s : static friction factor = 1.0
μ_k : kinematic friction factor = 0.45

• Vegetation Model

For modeling the effect of vegetation, the following equation is included in the model,

$$\frac{F_v}{\rho} = \frac{1}{2} C_{dv} \lambda_v \left(u^2 + v^2 \right) hv \quad (15)$$

where:

F_v : drag force due to vegetation;
C_{dv} : drag coefficient;
λ_v : vegetation density; and
h_v : water depth or vegetation height, Fig. (3).
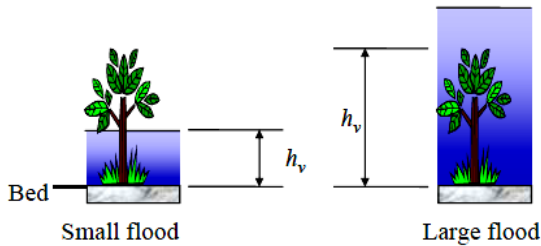
Fig. (3): Indication of term h_v used in vegetation model.

where,

$$\lambda_v = \frac{nd}{s^2} \quad (16)$$

s^2 is the area of grid cell, n is the number of stems of vegetation in the cell, d is the averaged diameter of each stem, Fig. (4).
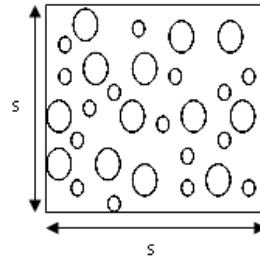
Fig. (4): Plan view of vegetation points.

• Grid Generation

The three dimensional model called IRIC (International River Interface Corporative), is a model used for supporting the numerical modeling of river morphodynamics using different turbulence models based on an explicit finite difference method (Abbott-Ionescu scheme) with upwind scheme.

The description of grid is given as:

• number of streamwise nodes = 501;
• number of cross-stream nodes in right and left floodplains = 5;
• number of cross-stream nodes in main channel = 25;
• number of iterations = 25; and
• standard relaxation coefficient = 0.2.

The basic goal of mesh design is creating a representation of the water body that provides an adequate approximation of the true solution of the governing equations.

The stage of network design is finished when the contour of the whole reach can be plotted by the program. The different

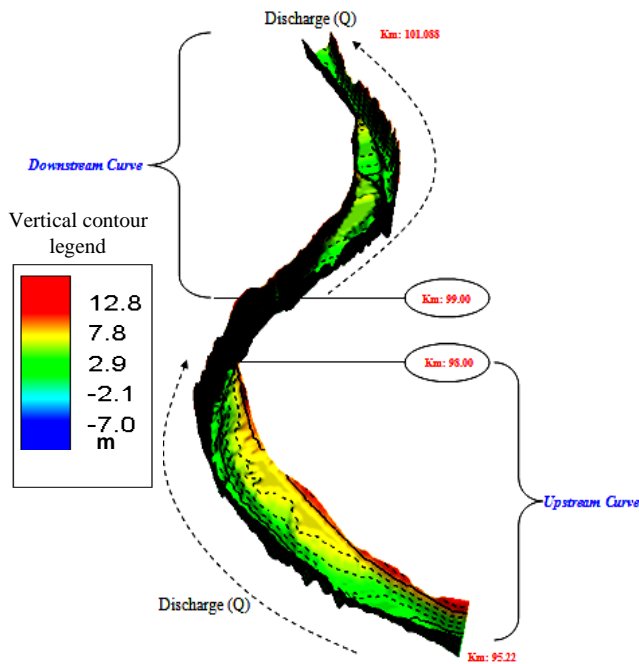grid elements for the whole reach could be plotted as given in Fig. (5).

Fig. (5): *3-D contour map for the reach under study.*

The following items have to be adjusted for all runs as:
• output time interval = 1 sec;
• calculation time step = 0.001 sec (minimum time step);
• start time for output = 0.0 sec;
• end of time steps calculations= 50 sec; and
• start time for bed deformation = 0.0 sec.
The boundary conditions can be specified for all runs as:
-no periodic boundary conditions;
-upstream velocity will be calculated according to uniform flow principles; and
-boundary condition slope will be estimated from geometric data.
-downstream water levels for measured, minimum, maximum and future discharges are 9.19 m, 8.37 m, 9.55 m and 10.51 m, respectively.
According to initial conditions; the initial water surface should be calculated according to the principles of non-uniform flow.
The median diameter of bed material (d_{50}) can be entered as a file with the extent of (.anc), and the standard value of critical angle of repose (φ) for bed material is used and equal to 0.3 (Shimizu, 2012).

In this model; both the length and width of the reach are divided into 500 and 32 units, respectively.

4. MODELING PROCESS

4.1- Case (1): Measured Flow –

• *Water velocity*

To determine reach zones subjected to maximum velocity and the scouring process, three longitudinal sections were selected. These sections are the most appropriate positions which could be obtained by the model, at 31.25% Bi, 62.5% Bi and 78.125% Bi, where Bi is the reach width at any cross section (i) measured from right bank to left bank, Fig. (6). Figs. (7) through (9) show the water velocity through these sections.
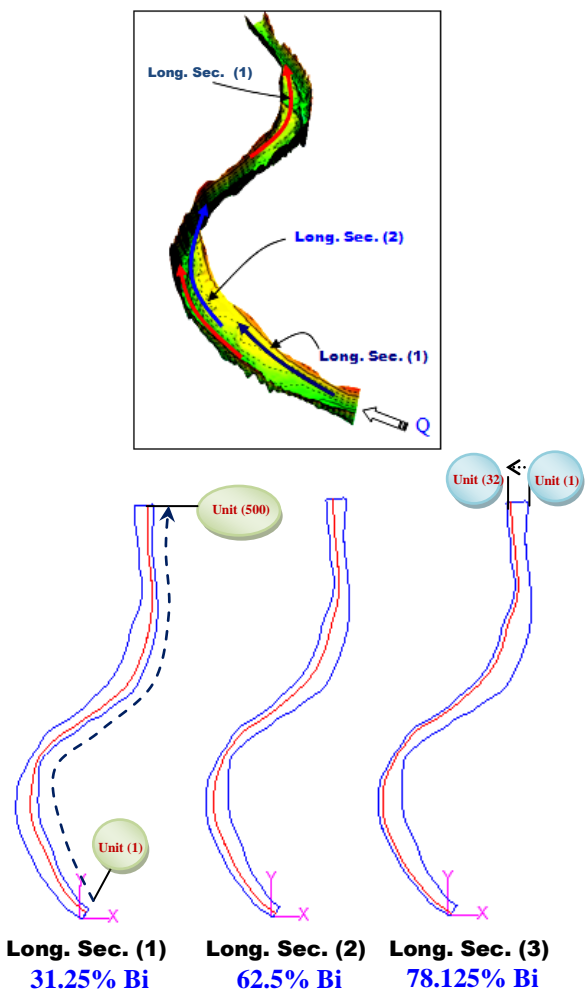
Fig. (6): *Locations of selected longitudinal sections.*
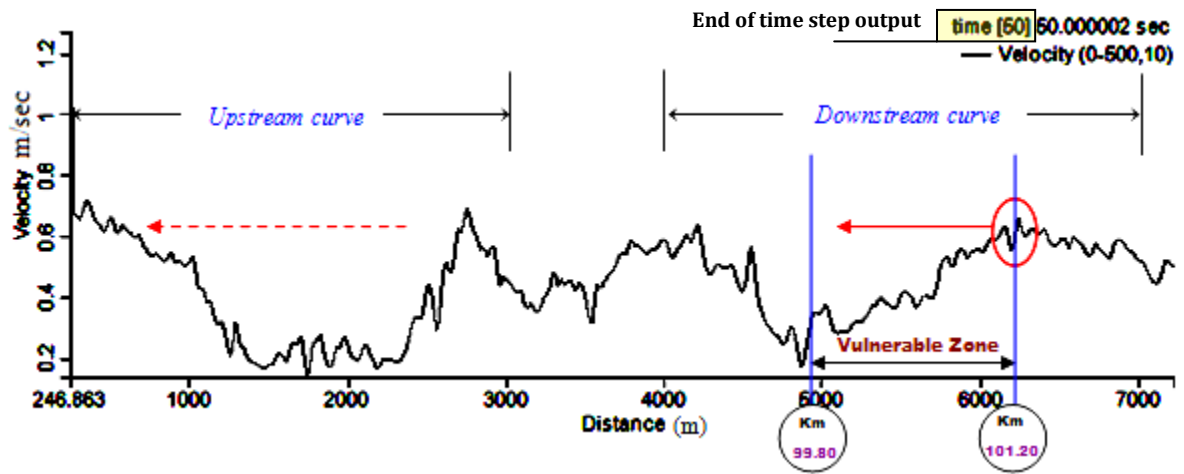
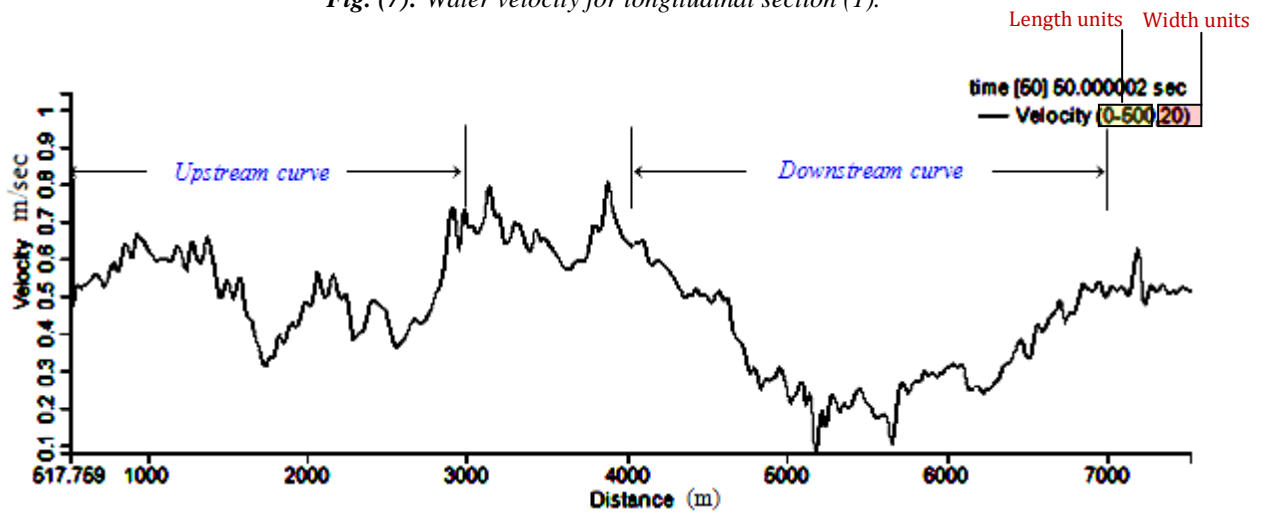*Fig. (7): Water velocity for longitudinal section (1).*

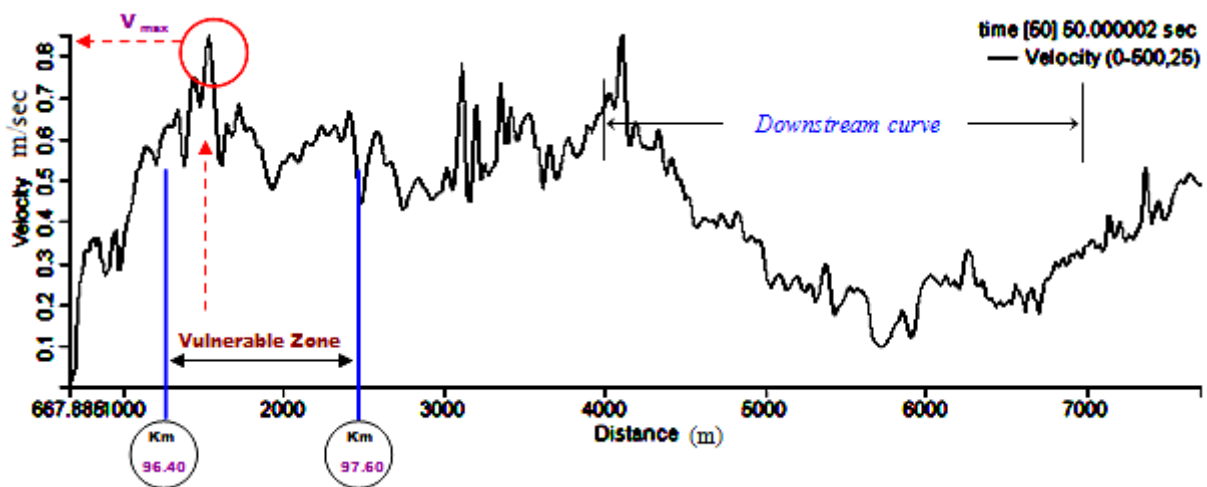*Fig. (8): Water velocity for longitudinal section (2).*

Fig. (9): Water velocity for longitudinal section (3).

From analysis of these figures, it can be observed that:

• The outer edge of the upstream curve is subjected to maximum velocity of 0.85 m/sec at km: 96.60 downstream of El-Roda gauge station;

• The vulnerable zone that needs a protection process for the upstream curve starts from km 96.40 to km 97.60, Fig. (9). This zone is defined as the most likely affected area by the direct impact of the scour process;

• For the downstream curve, the vulnerable zone is found between km 99.80 to km 101.20 downstream of El- Roda gauge station;

• The maximum water velocity at the outer edge of the downstream curve is 0.63 m/sec at km: 101.20 downstream El- Roda gauge station; and

• The value of velocity at the straight part, located between the upstream and downstream reach curves, from km: 98.00 to km: 99.00 ranges from 0.35 m/sec to 0.81 m/sec. It was found that these values are located in the middle of the reach.

For showing the water velocities along river width through the whole reach, the velocities of selected eight cross sections along the width of reach at km:95.220, km:96, km:97, km:98, km:99, km:100, km:101 and km:102, Fig. (10), are illustrated from Figs. (11.1) through (11.8). The horizontal axis of these Figs. refers to the distance in meters measured from the right bank to the left bank.
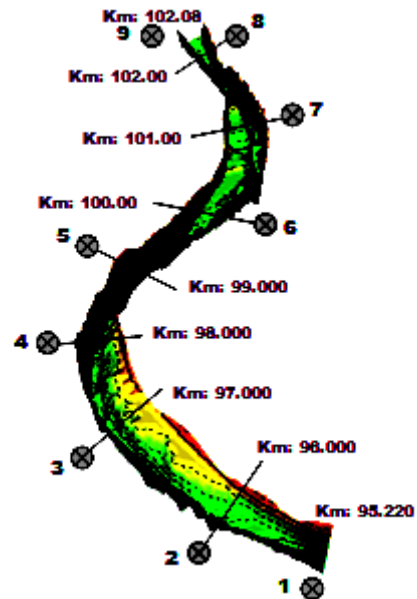
Fig. (10): Locations of the selected cross- sections.
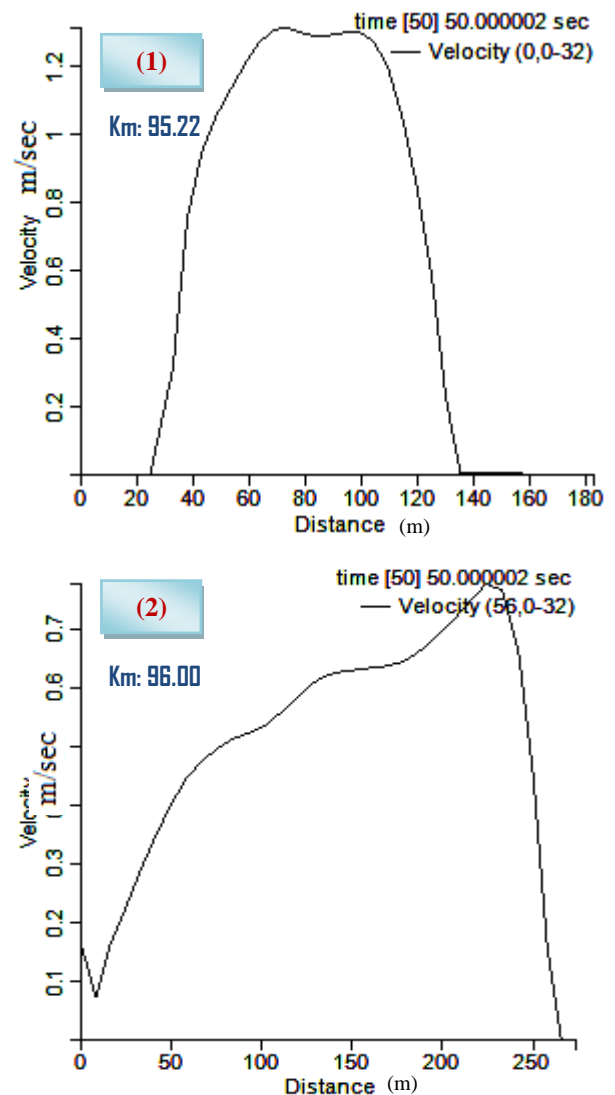
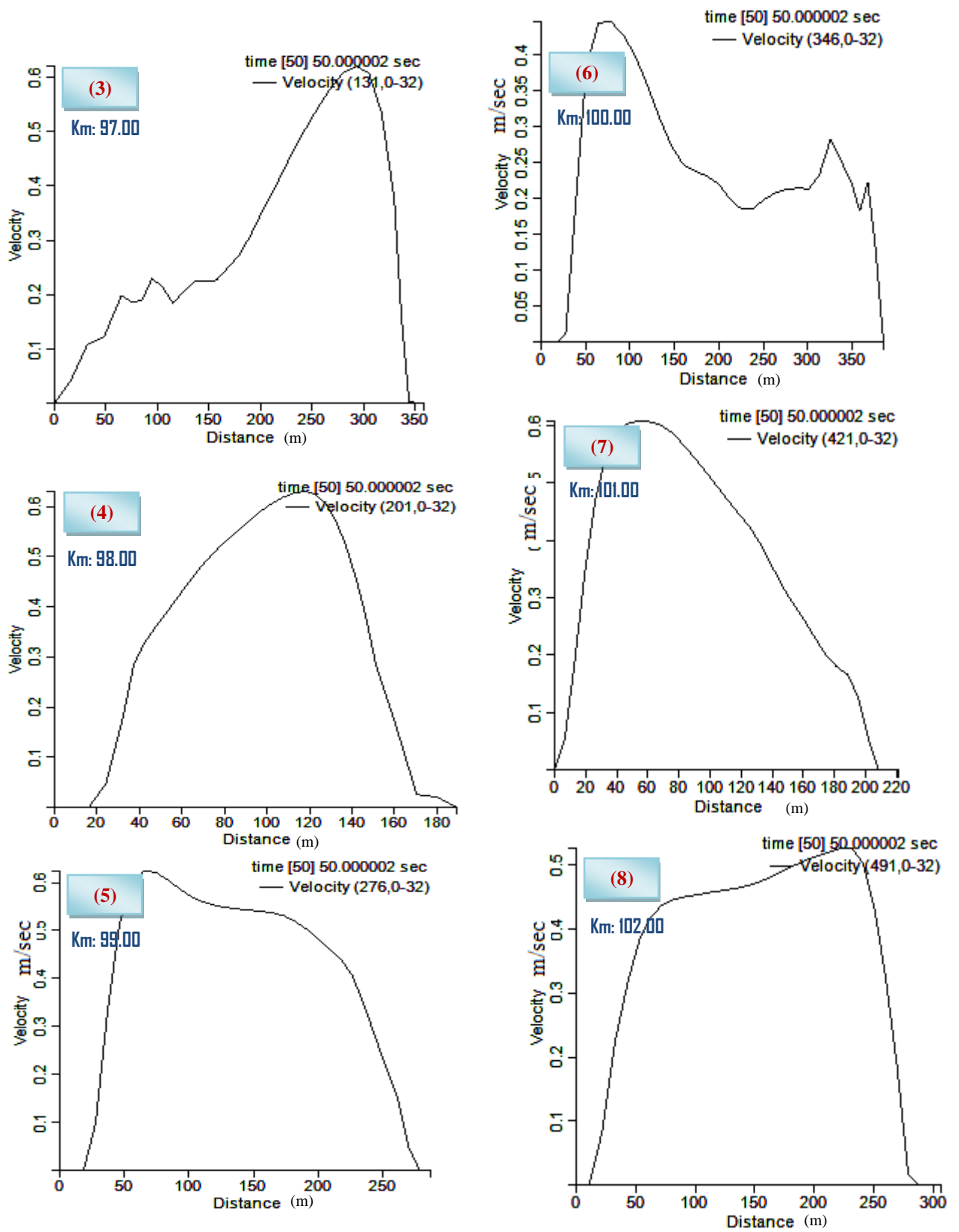*Fig. (11): Velocity distribution along river width at (1) Km: 95.22, (2) Km: 96.00*

Fig. (11): *Velocity distribution* *continued* *at (3) Km: 97.00, (4) Km: 98.00, (5) Km: 99.00, (6) Km: 100.00, (7) Km: 101.00, and (8) Km: 102.00.*

It can be concluded from analysis of the previous velocity profiles that:

• The maximum velocity occurs through the whole reach is 1.3 m/sec at km: 95.220 (beginning of the study reach) at 65 m far from the right bank; and

• The inner edges for the upstream and downstream curves are subjected to lower velocity ranges from 0.05 m/sec to 0.1 m/sec, these values may cause sedimentation process.

The outer edges for the upstream and downstream curves are subjected to the maximum velocity values due to the centrifugal force of water body at these curves. This centrifugal force compelled the water level not only through the river width but also the whole reach to change from point to another. For this reason, it is important to find out the water surface elevation change.

The largest flow velocities in mildly curved flow are found at the outside of the curved flow, e.g. the outer bend in curved river flow.

The mechanism that makes the flow velocity at the outside of the curvature increase at the expense of the velocity at the inside is differential advection, which can be understood as follows: in mildly curved flow the main flow velocity profile over the vertical is almost logarithmic. Hence the centrifugal force due to the curvature of the flow is larger in the upper part of the flow than near the bottom.

On the average, this centrifugal force is compensated by the pressure gradient due to a surface slope towards the outer bend. The resulting force is directed to the outward side in the upper part of the flow and to the inward side near the bottom and hence leads to a secondary flow to the outside in the upper part and to the inside near the bottom, Fig. (12).

Both the main and the secondary flows form the helical flow observed in the curved parts.

In mildly curved flow, the amount of water flowing outward is more or less equal to the amount of water flowing inward. However the main flow velocity is larger in the upper part of the flow than in the lower part, hence more main flow momentum is transported outwards in the upper part of the flow than inwards in the lower part. This leads to a net transport of main flow momentum in outward direction and consequently to higher flow velocities at the outer bend.
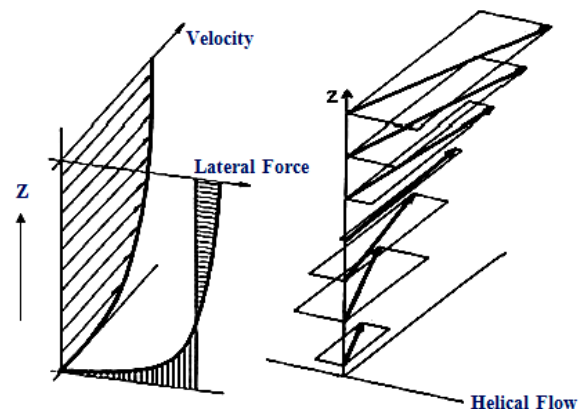

Fig. (12): Mechanism of differential advection.

• **Water surface elevation**

This part shows the variation of water surface elevation through the whole reach especially through the reach edges. The water surface elevation for the three selected longitudinal sections, Fig. (6), at 31.25% Bi, 62.5% Bi and 78.125% Bi, are given from Figs. (13) through (15).
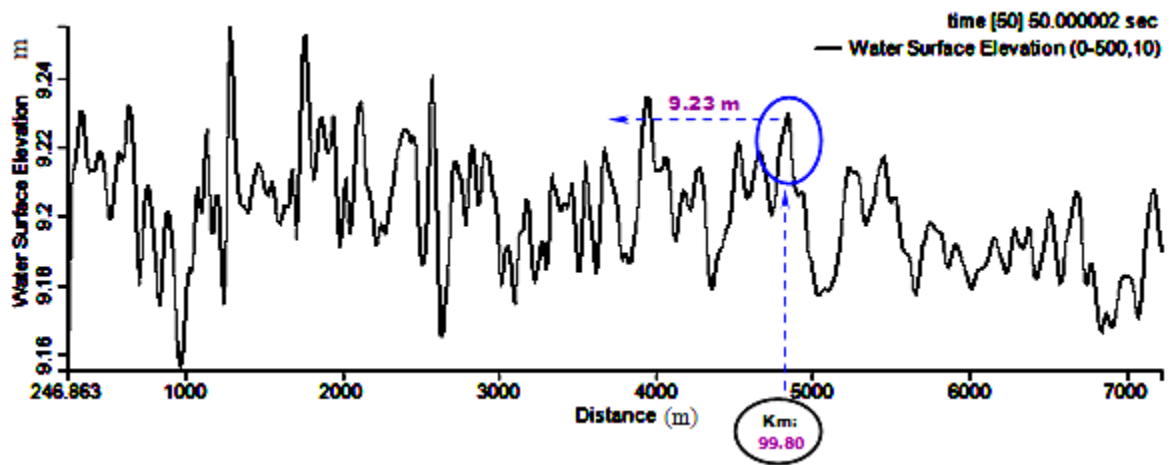
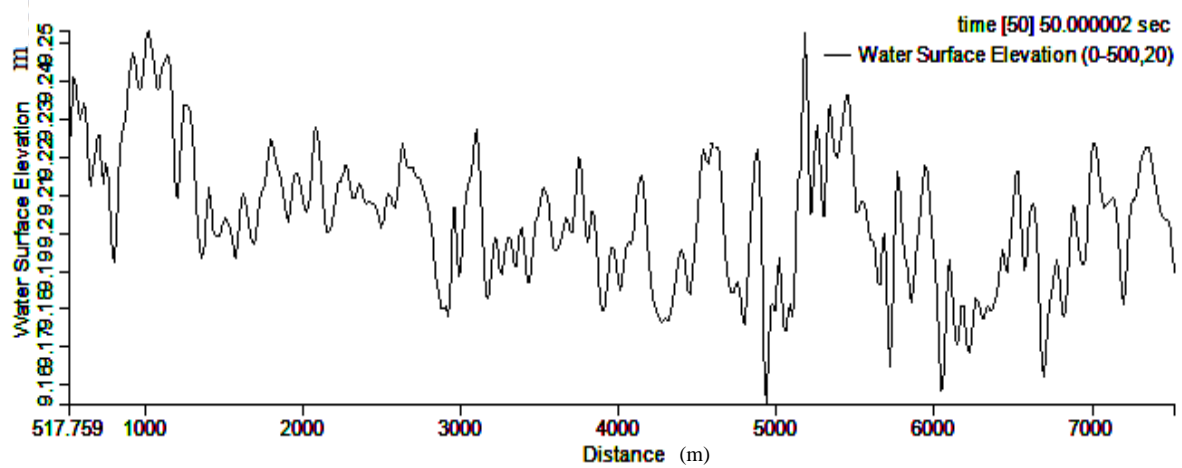***Fig. (13):*** *Water surface elevation for longitudinal section (1).*

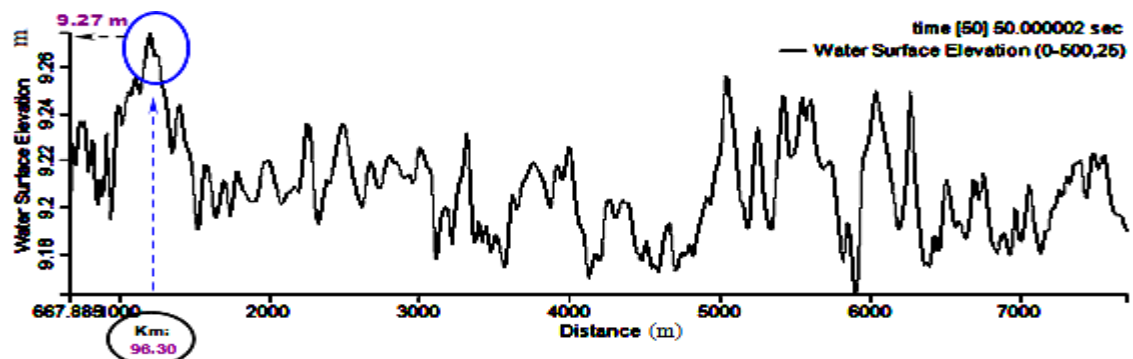***Fig. (14):*** *Water surface elevation for longitudinal section (2).*

Fig. (15): *Water surface elevation for longitudinal section (3).*

From these figures, it can be noticed that:

• The maximum water surface elevation for the upstream curve is 9.27 m at km: 96.30;

• The water surface elevation for the downstream curve is 9.23 m at km: 99.8; and

• The value of water surface elevation at the straight part, between the upstream and downstream curves from km: 98.00 to km: 99.00, ranges from 9.148 m to 9.24 m. This value is found at the middle of the reach width not at the reach edges.

It is observed from the previous figures that the water surface increases gradually from the inner curve to the outer curve at the upstream and downstream curves, this is due to the centrifugal force.

• *bed deviation*

Change of water velocity and change of water surface elevation and difference in bed topography result in different deviations along the whole reach. This deviation in bed elevation occurs in both the direction of flow, longitudinal direction, and through the transverse direction.

Longitudinal bed deviations are illustrated through five selected longitudinal sections, at 31.25% Bi, 46.875% Bi, 62.5% Bi, 78.125% Bi and 93.75% Bi, where Bi represents the reach width at any cross section (i) measured from right bank to left bank, Fig. (16).

Figs. (17) through (21) show the deviation of bed elevation for these sections due to using bed load model only.
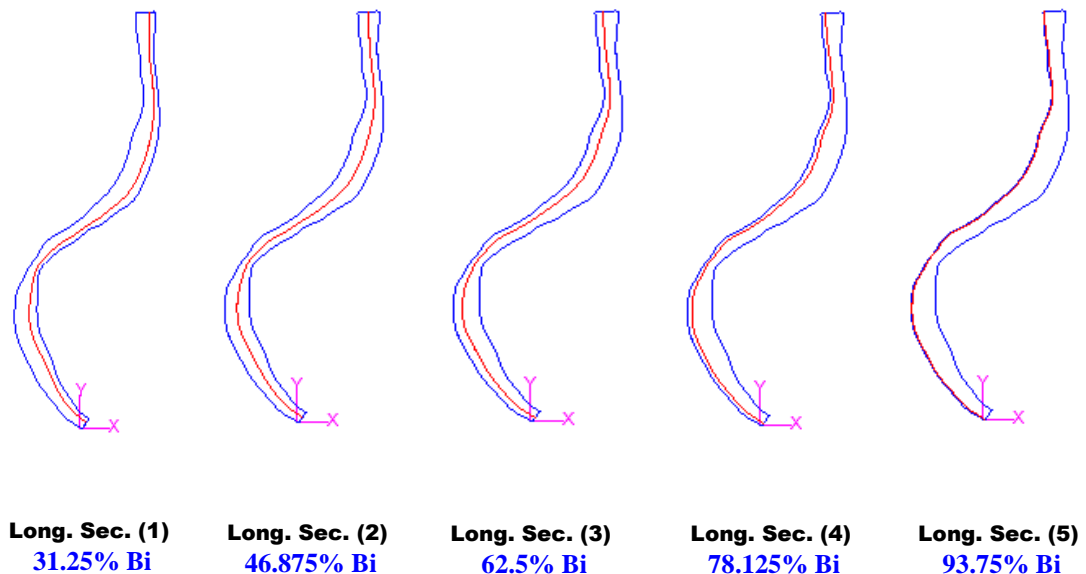

| Long. Sec. (1) | Long. Sec. (2) | Long. Sec. (3) | Long. Sec. (4) | Long. Sec. (5) |
| 31.25% Bi | 46.875% Bi | 62.5% Bi | 78.125% Bi | 93.75% Bi |

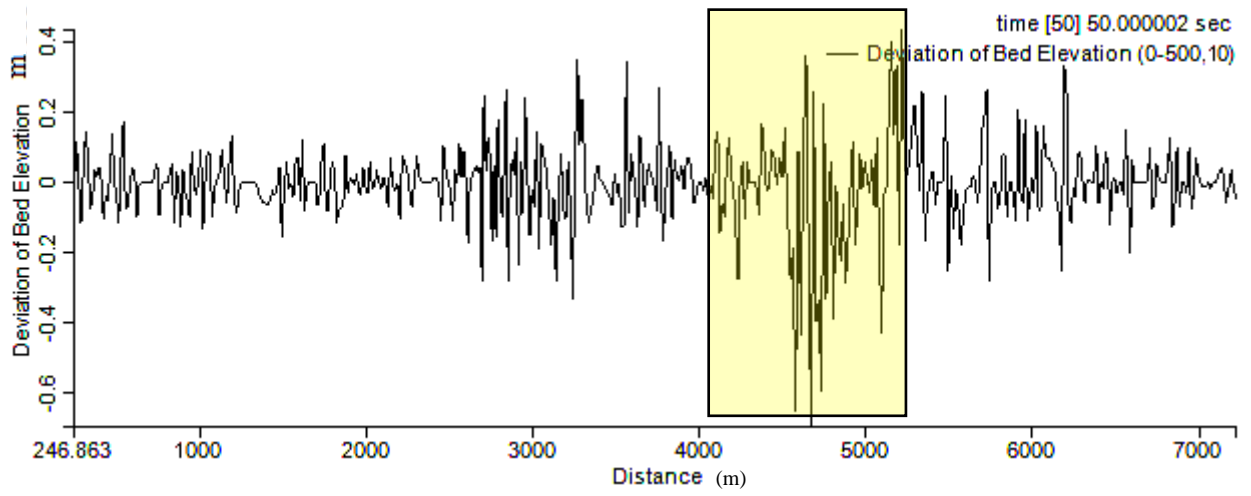*Fig. (16): Location of the five selected longitudinal sections.*

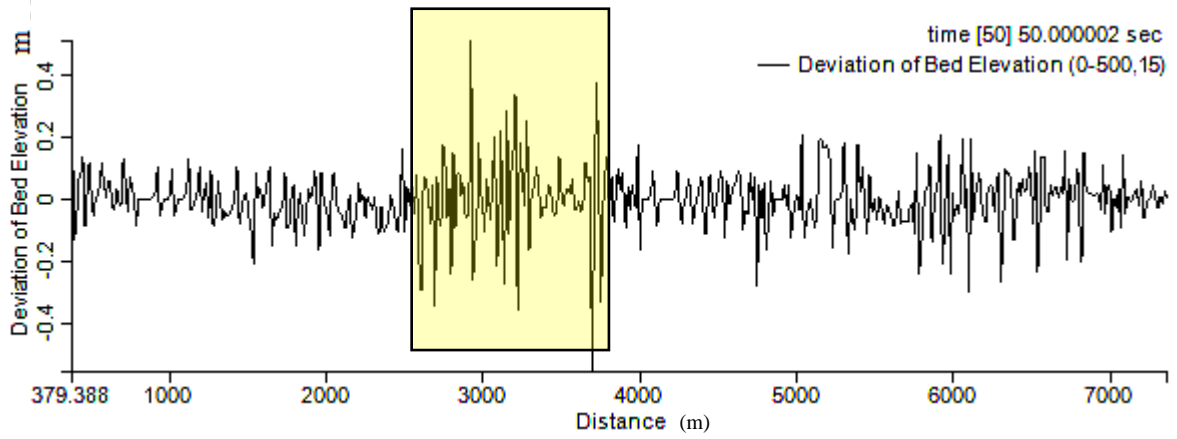*Fig. (17): Deviation of bed elevation for longitudinal section (1).*

Fig. (18): Deviation of bed elevation for longitudinal section (2).
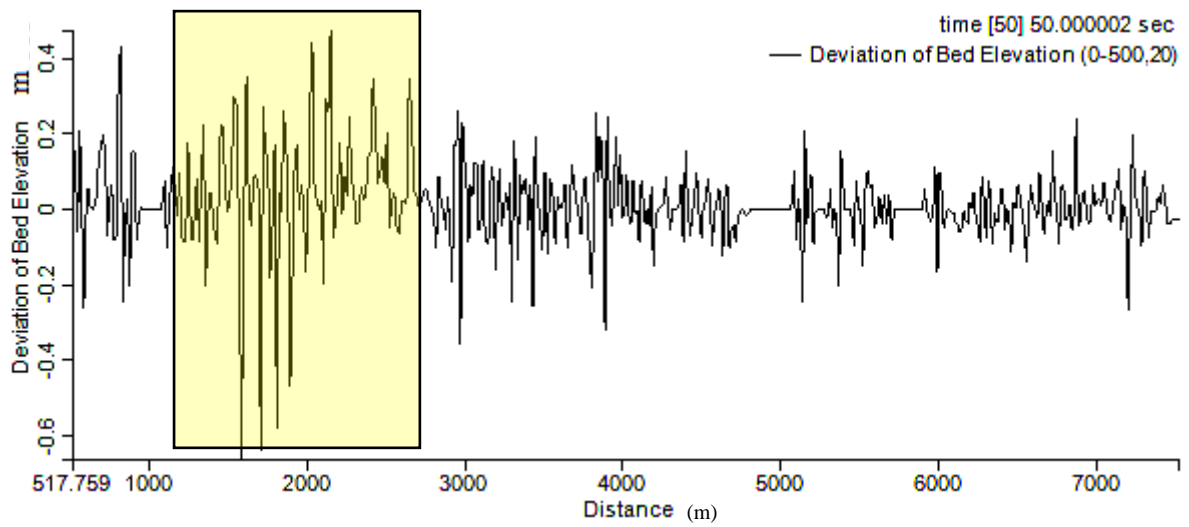

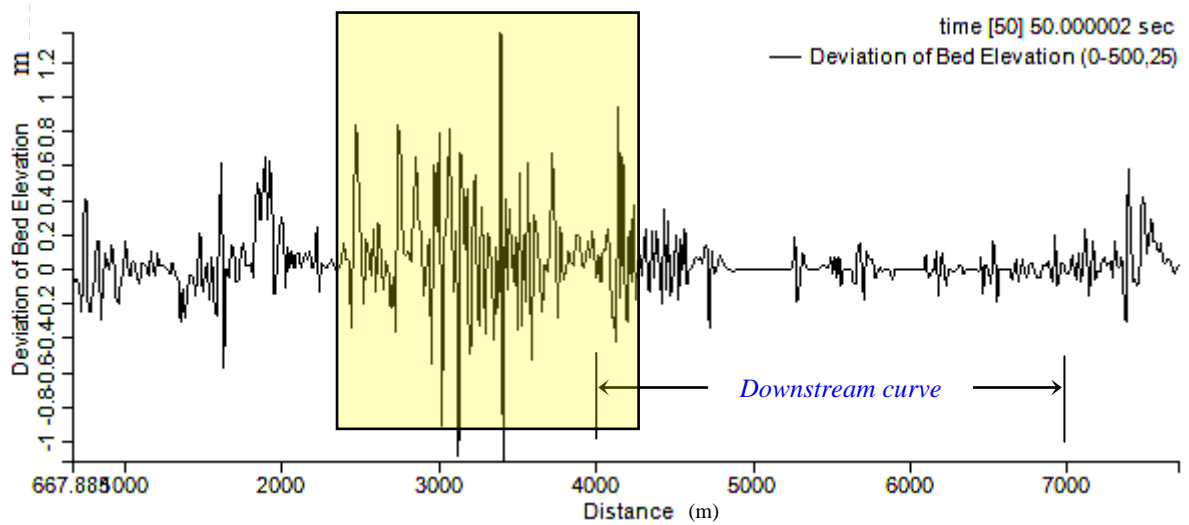*Fig. (19): Deviation of bed elevation for longitudinal section (3).*

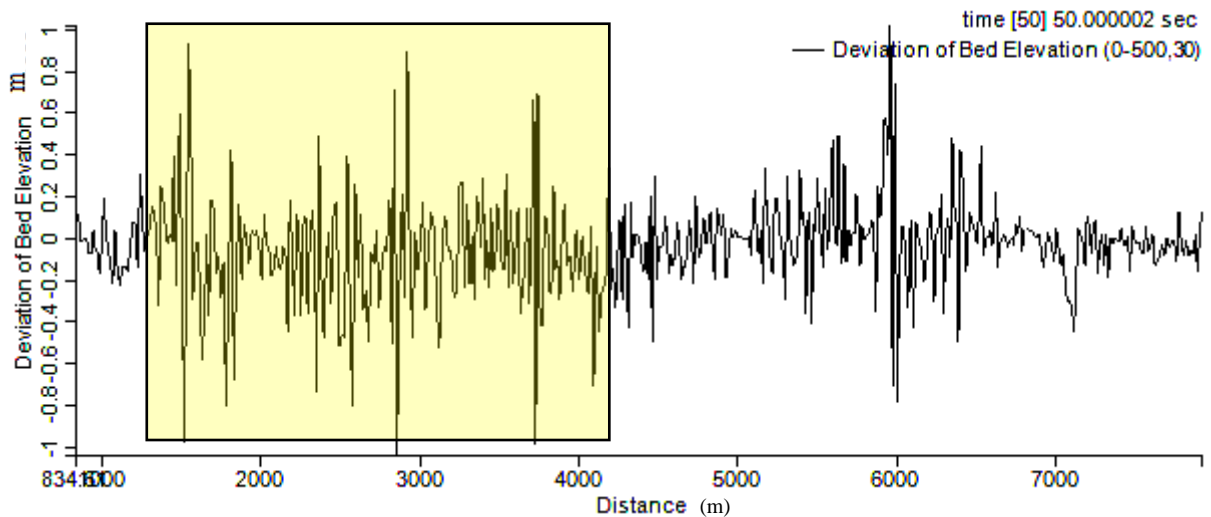*Fig. (20): Deviation of bed elevation for longitudinal section (4).*

Fig. (21): Deviation of bed elevation for longitudinal section (5).

From analysis of the previous figures, it can be concluded that:

•Bed elevation changes from point to another and from zone to another along the length of the reach according to the current flow characteristics;

• The maximum value of bed deviation for the upstream curve at the outer edge ranges from -0.9 m to + 0.8 m at km: 96.5 to km: 97.00; and

• For the downstream curve at the outer edge, the maximum value of bed deviation ranges from -0.60 m to + 0.40 m at km: 99.00 to km: 101.00.

These actions could be explained as the centrifugal force for the upstream curve is greater than that occurs in the downstream curve.

4.2- Case (2): Minimum Flow –

According to River Transport Authority data for Damietta branch, the maximum width of navigation waterway is 40 m and the safe maximum draft is 2.30 m as a one way navigation channel. There are dredging works every year for this branch with higher cost.

Consequently, the navigation consideration is the most important condition which has to be studied using minimum discharge as the water depth of the river must cover the minimum consideration of the maximum draft of any navigation unit passes through Damietta branch (2.3 m) so, it is important to simulate the water depth and velocity through the reach to study the sedimentation zones throughout the reach.

- *Velocity and water depth*

Figs. (22) and (23) demonstrate the water velocity and water depth filled contours for the whole reach to find out points of sedimentation and minimum velocity value, which occur through the whole reach.
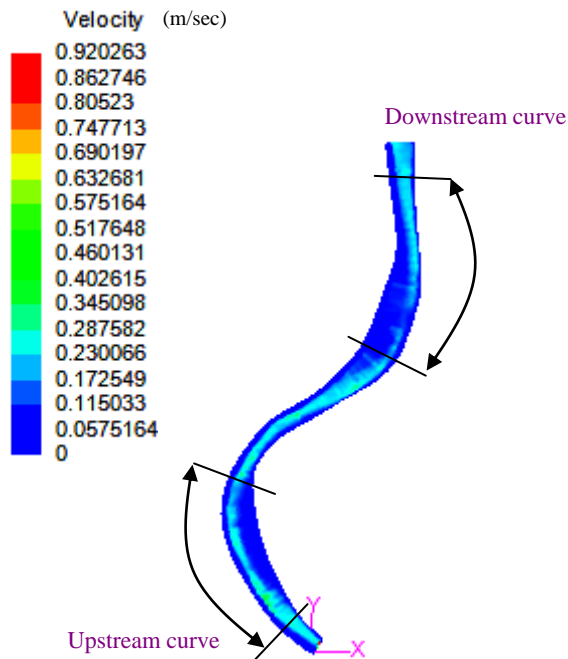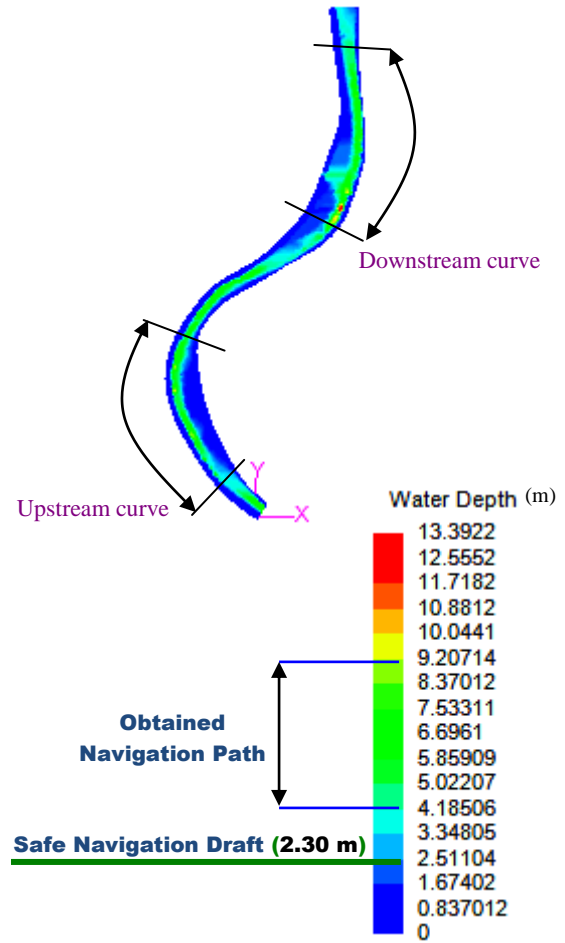

Fig. (22): Velocity contours.

Fig. (23): Water depth contours.

From these figures, it is observed that:

- The minimum velocity values of 0.03 m/sec and 0.01 m/sec occur at the inner edges for the upstream and downstream curves respectively, and the maximum ones occur at the outer edges having values of 0.3 m/sec and 0.2 m/sec for the upstream and downstream curves, respectively;
- The velocity at the downstream curve is less than the corresponding one at the upstream curve. This may cause more sedimentation at downstream curve; and
- The navigation waterway resulted from the model (the same green color waterway shown in Fig. (23)) is wider than the waterway obtained from River Transport Authority.

The resulted waves from moving the navigation units through the waterway, Fig. (23), cause more erosion through the outer edges of the upstream and downstream curves. It could be concluded that the outer edges of the reach have to be protected using any suitable structure.

As longitudinal section (2) is far from the reach edges, Fig. (6), it is convenient to study longitudinal sections (1) and (3).

The water velocity and the corresponding water depth for the same selected longitudinal sections (1) and (3), Fig. (6), are demonstrated in Figs. (24) and (25).
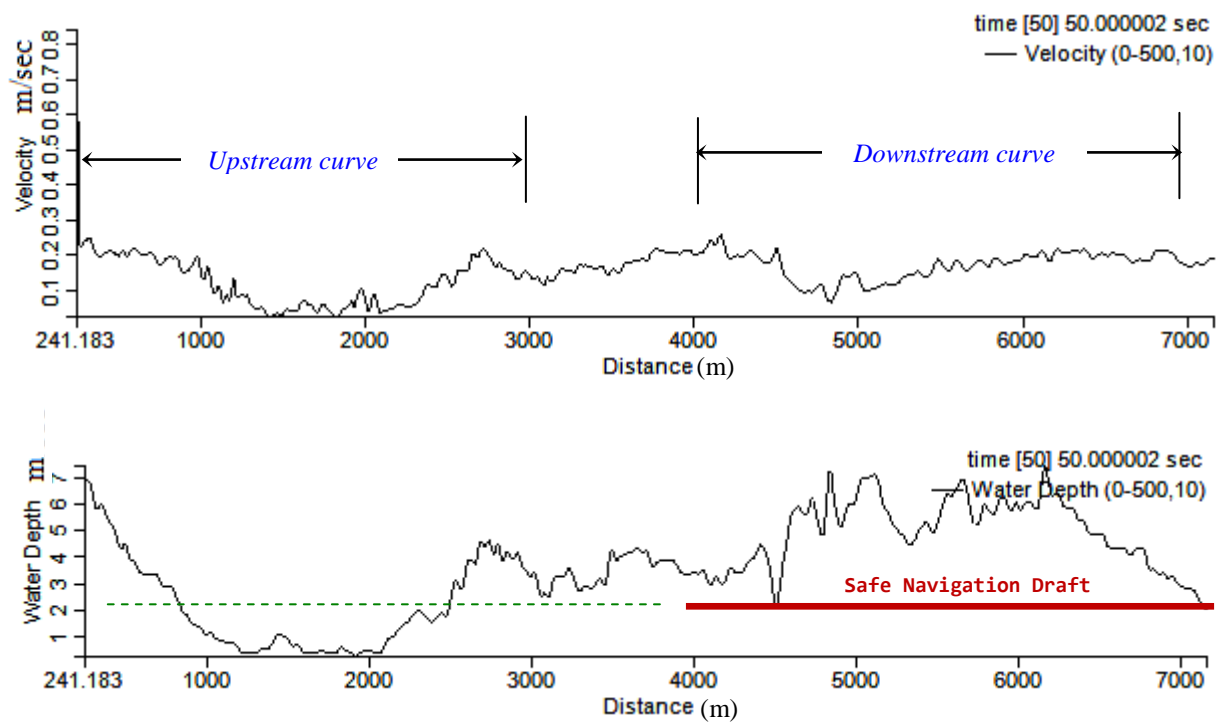

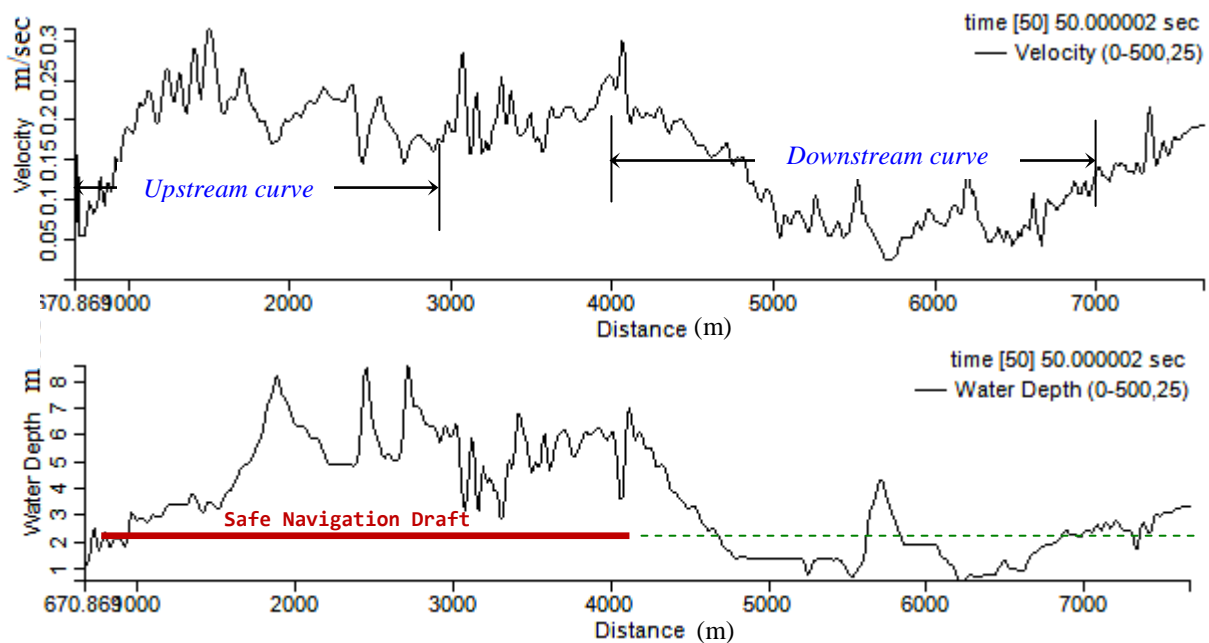Fig. (24): Velocity and water depth for longitudinal section (1).

Fig. (25): Velocity and water depth for longitudinal section (3).

4.3- Case (3): Maximum Flow –

Modeling the reach using the maximum discharge (Q_{max} = 718.75 m³/sec) occurred through past years, could be useful to describe the flow conditions and bed deviations through zones subjected to higher values of water velocity.

- ▪ *Velocity and water surface elevation*

Water velocities and the corresponding water surface elevations for longitudinal sections (1) and (3) are shown in Figs. (26) and (27).
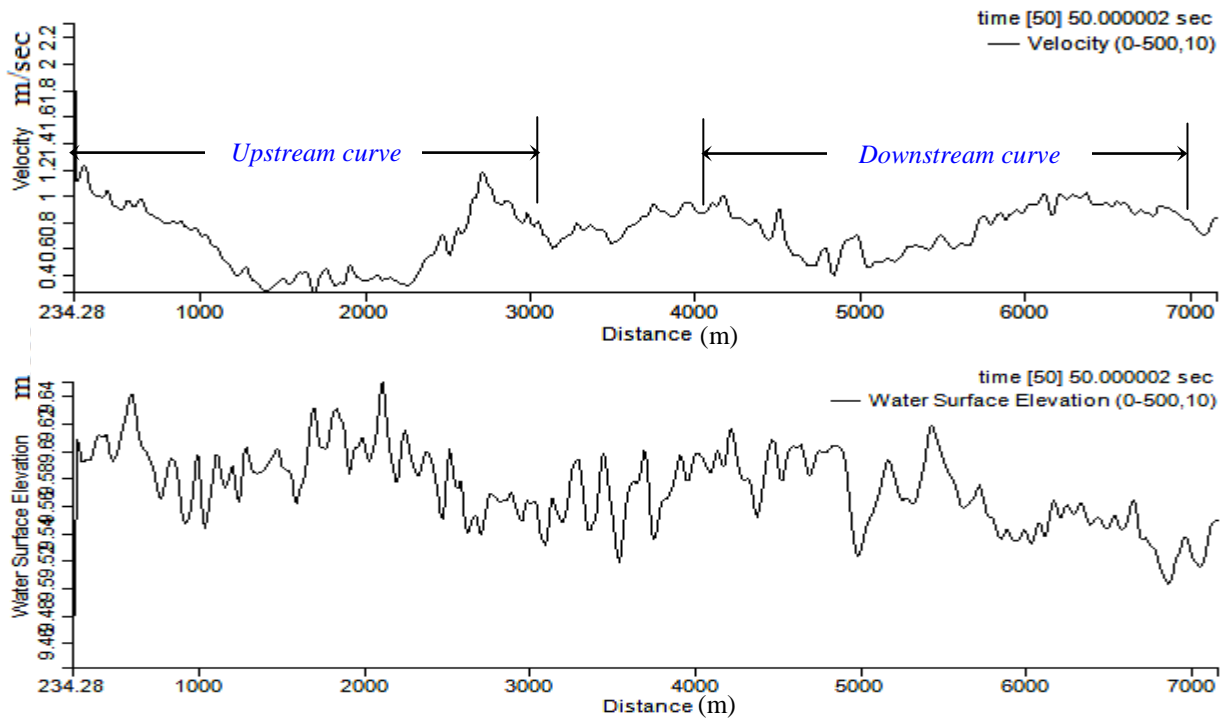

Fig. (26): *Water velocity and surface elevation for longitudinal section (1).*
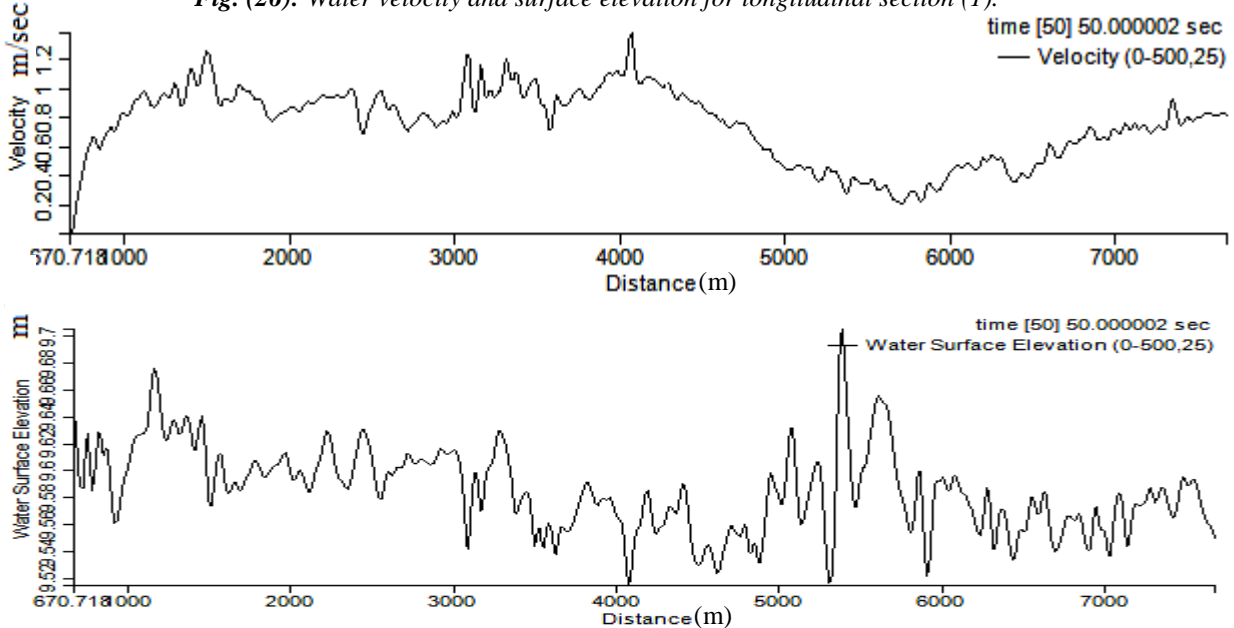

Fig. (27): *Water velocity and surface elevation for longitudinal section (3).*

Analysis of these figures indicates that:

• The outer edge of the upstream curve is subjected to maximum velocity of 1.2 m/sec at km: 96.50;
• The maximum velocity of water at the outer edge of the downstream curve is 1.0 m/sec at km: 101.00;
• The inner edges for both the upstream and downstream curves are subjected to lower velocity, its value ranges between 0.05 m/sec and 0.2 m/sec, which may cause a sedimentation processes;
• The water surface elevation increases gradually nearby the outer edges for the upstream and downstream curves; and

• The maximum values of water surface elevation for both the upstream and downstream curves are 9.68 m at Km: 96.50 and 9.65 m at km 100.50, respectively.

4.4- Case (4): Future Flow –

The future discharge is defined as future peak discharge for Damietta branch rehabilitation. (120 M.m^3/day)

• *Water velocity*

Figs. (28) and (29) illustrate the water velocity for longitudinal sections (1) and (3), Fig. (6), along the reach under study.
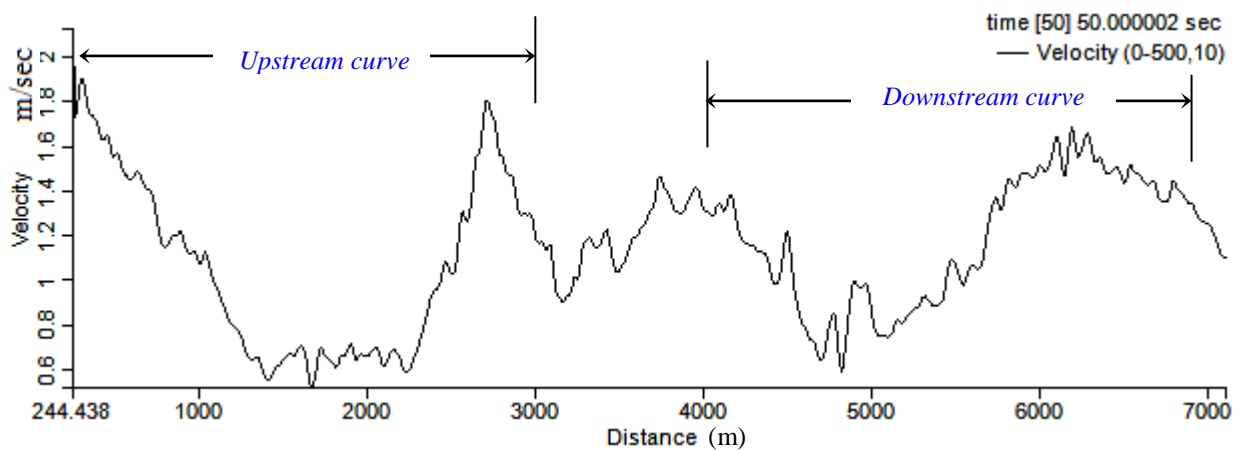

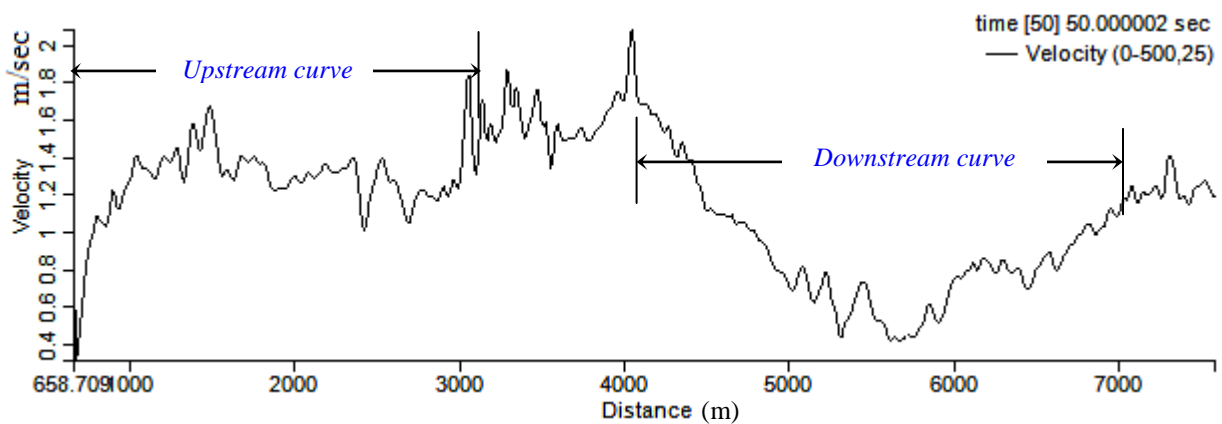*Fig. (28): Water velocity for longitudinal section (1).*

Fig. (29): Water velocity for longitudinal section (3).

From the aforementioned figures, it is observed that:

• The upstream and downstream curves are subjected to maximum velocity of 1.6 m/sec at km: 96.50 and 1.5 m/sec at km: 101.00;
• The value of velocity for the straight part of the reach, between the upstream and downstream curves, varies between 1.2 m/sec and 2.2 m/sec, and the positions of these values are in the middle in this part; and
• The maximum velocity occurs through the whole reach is 2.2 m/sec at km: 99.00.

• *Vorticity and water depth*

Figs. (30) and (31) exhibit the water vorticity (sec^{-1}) and corresponding water depth for the abovementioned two longitudinal sections.
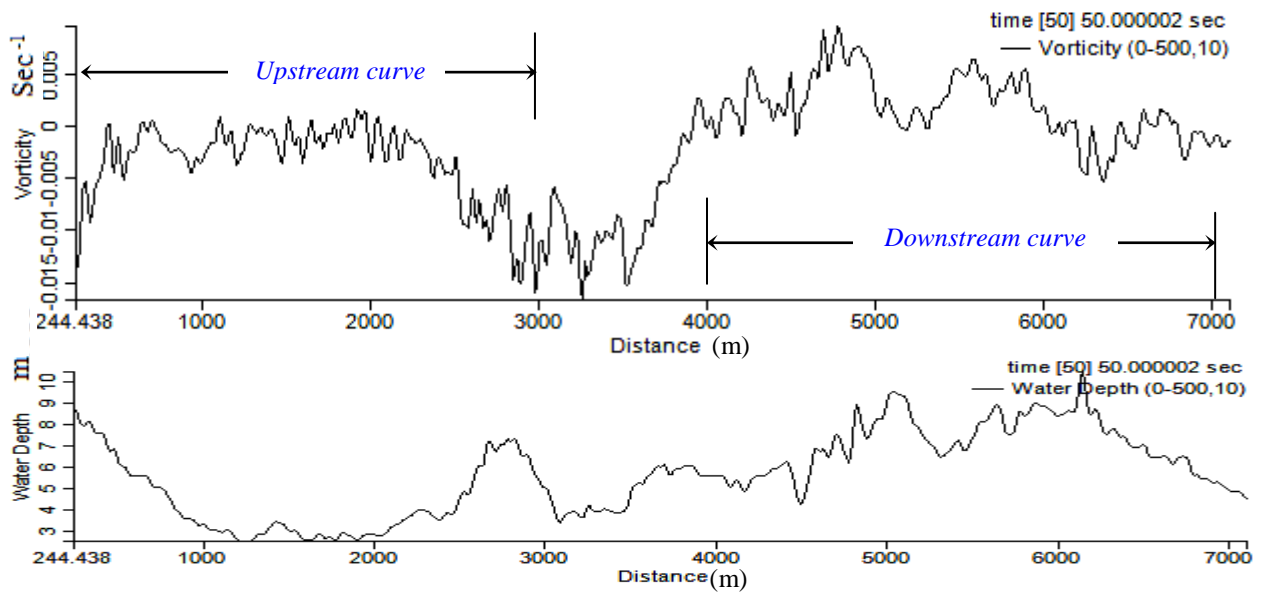

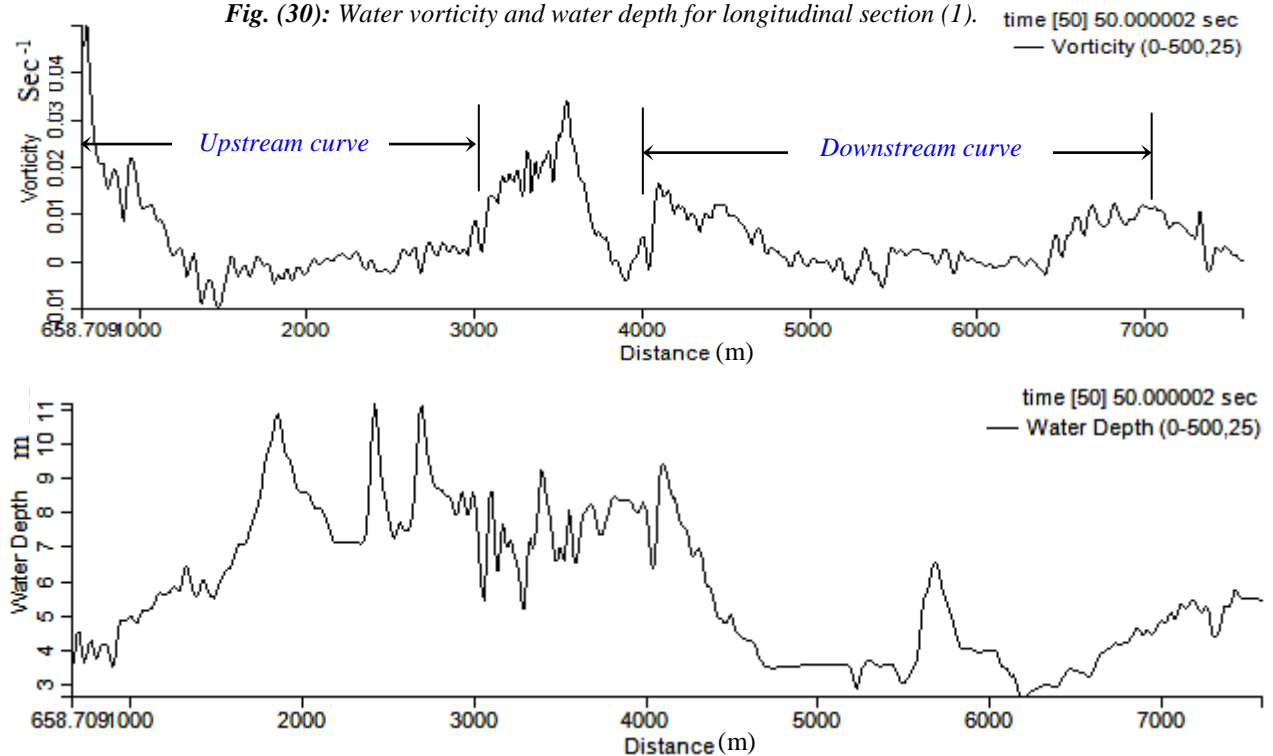***Fig. (30):*** *Water vorticity and water depth for longitudinal section (1).*

Fig. (31): *Water vorticity and water depth for longitudinal section (3).*

From analysis of these figures, it can be concluded that:

• Turbulence of water at the upstream curve is more than that occurs at the downstream curve;
• Vorticity through the reach ranges from -0.099 sec^{-1} to + 0.035 sec^{-1}; and
• The maximum value of vorticity occurs from km: 98.00 to km: 99.00.

5. CONCLUSIONS

The following conclusions are drawn from this research work:

• The vulnerable zone that needs to be protected for the upstream curve lies between km 96.40 and km 97.60. This zone is defined as the most likely affected area by the direct impact of the scour process;
• For the downstream curve, the vulnerable zone is found between km 99.80 to km 101.20;
• The maximum water surface elevation for the upstream curve is 9.27 m at km: 96.30 in case of measured flow;
• The water surface elevation for the downstream curve is 9.23 m at km: 99.8 in case of measured flow;
• The water surface increases gradually from the inner curve to the outer curve at both the upstream and downstream curves. This increasing value in water level near the outer curve is due to the centrifugal force;
• The navigation waterway resulted from the model is wider than that obtained from River Transport Authority;
• The upstream and downstream curves are subjected to maximum velocity of 1.6 m/sec at km: 96.50 and 1.5 m/sec at km: 101.00 in case of future flow;
• The value of velocity for the straight part of the reach, between both the upstream and downstream curves, varies between 1.2 m/sec and 2.2 m/sec, it is found in the middle of the reach around the centerline in case of future flow;
• The maximum velocity occurs through the whole reach is 2.2 m/sec at km: 99.00 (the straight part) in case of the expected future flow; and
• Turbulence of water at the upstream curve is more than the turbulence at the downstream curve.

ACKNOWLEDGMENTS

REFERENCES

[1] Ahmed A. F. (2010). "Improving navigation in river bends by bottom vanes", Scientific Bull., Faculty of Engineering, Ain Shams University, ISSN 1110-1385, Vol. 32, No. 1.

[2] Attia K. M. and El-Saied N.A. (2004). "Plan form geometry of river meander at Damietta branch", Scientific Bulletin, Faculty of Engineering, Ain Shams University, ISSN 1110-1385, Vol. 39, No. 1, pp.359-379.

[3] Grade R. J. (1995). "History of fluvial hydraulics", New Age Publishers. p. 14.and p.19, ISBN 812240815X. OCLC 34628134.

[4] Hickin J.S. (2003). "Meandering channels", International Journal of Recent Trends in Engineering, India, Vol. 1, No. 6, pp. 430–434.

[5] Inglis C.D. (1938). "Relationship between meander belts", Central Irrigation Hydrodynamic, India, Tech. Note No. 12.

[6] Leopold L. B. and Wolman M. G. (1960). "River meanders", Geological Society, Bull., Vol. 71, pp. 769-794.

[7] Leopold L. B., Wolman M. G., and Miller J. P. (1964). "Fluvial processes in geomorphology", W. H. Freeman, San Francisco, California.

[8] Shimizu Y.R., Itakura T.G., and Yamaguchi H.K. (1990). "Three dimensional computation of flow and bed deformation", Journal of Hydraulics, ASCE, Vol.116, No. 9, pp. 1090-1108.

[9] Shimizu Y.R. (2012). Lecture Notes, "3-D river hydraulics modeling", Hokkaido University, Japan.

[10] Wang S.S. (1988). "Three dimensional models for fluvial hydraulic simulation", Proceeding of the International Conference on Fluvial Hydraulics, Budapest, Hungary, 88-30.

[11] Wang S.S., Combs P.X., and Hu K.K. (1989). "New developments in modeling 3D sedimentation phenomena", New Orleans, Louisiana, Vol.14, No.18, pp. 33-38

[12] Zeller J.D. (1967). "Meander channels in Switzerland", Cranfield University Report, Britannia.